Effective coupling of phenol adsorption and photodegradation at the surface of micro-and mesoporous TiO2-activated carbon materials

C. Telegang Chekem, Y. Richardson, M. Drobek, Gaël Plantard, J. Blin, V. Goetz

Effective coupling of phenol adsorption and photodegradation at the surface of micro-and mesoporous TiO_2-activated carbon materials

C. Telegang Chekem[(1)(2)],Y. Richardson[(1)*], M. Drobek[(3)],G. Plantard[(2)], J. Blin[(1)(4)], V. Goetz[(2)]

[(1)]Institut International d'Ingénierie de l'Eau et de l'Environnement (2iE), Laboratoire Biomasse Energie et Biocarburants (LBEB), Rue de la Science, 01 BP 594, Ouagadougou 01, Burkina Faso

[(2)]PROMES-CNRS UPR 8521, PROcessMaterial and SolarEnergy, Rambla de la Thermodynamique 66100 Perpignan, France

[(3)]Institut Européen des Membranes, UMR 5635, Université de Montpellier, ENSCM, CNRS, Place Eugène Bataillon, F-34095 Montpellier cedex 5, France

[(4)] CIRAD, UPR BioWooEB, F-34398 Montpellier, France

***corresponding author: richardson.yohan@gmail.com**

Abstract

Novel titania supported activated carbon catalysts were prepared by a straightforward titania coating route of a microporous activated carbon (AC) derived from shea nut shells, and investigated in phenol photocatalytic degradation. The proposed coating method enables a fixation of the preformed titania anatase nanoparticles (TiO_2 NPs) in the external porosity thus allowing their accessibility towards UV irradiation, without causing any reduction of the AC specific area. Interestingly, the coating treatment reshapes the porous texture of the as-prepared TiO_2-AC composite materials resulting in an improvement of the adsorption capacity and the formation of an additional mesoporosity on the AC surface. Photocatalytic experiments carried out in batch reactor led to 97% elimination rate of phenol in an aqueous solution with the AC catalysts containing TiO_2 NPs in the range from 11 to 34 wt %. The photodegradation performance of the TiO_2-AC catalysts was maintained over several successive cycles, without the need of any regeneration treatment. Considering both the textural and microstructural features of the composite materials and their associated phenol removal kinetics, in this paper we provide new insights into phenol photodegradation pathway involving an effective coupling of adsorption and photodegradation functionalities, resulting in a photo-assisted regeneration mechanism of the catalyst.

Keywords: Activated carbon; TiO_2 nanoparticles; Composite materials; Photocatalysis; Adsorption; Catalyst regeneration.

1. Introduction

Advanced Oxidation Processes (AOPs) are currently considered among the most efficient technologies to remove biorefractory micropollutants from water that cannot be eliminated by conventional techniques [1–3]. They allow the *in situ* generation of highly reactive species that induces the mineralization of pollutants. In heterogeneous photocatalytic AOP, reactive species like hydroxyl radical (•OH) get formed at the surface of a photoactive materials through reactions of electron donors and electron acceptors with electronic charge carriers (e^-/h^+) generated by light radiation. The as-formed reactive species drive the reactions of degradation of many organic pollutants, in particular those with the highly resistant aromatic rings down to smaller linear molecules and/or minerals [4]. Titania (TiO_2) has been reported in the literature as one of the best photocatalyst material and remains the subject of current intense research interest [5–9], although revealing numerous operational drawbacks [3, 10, 11] often associated with (i) tremendous and expensive catalyst post separation given the nano size of TiO_2 particles [3], (ii) partial degradation of the pollutants that may lead to the formation of intermediary harmful compounds, and (iii) the limitation in solar-powered applications owing to both the intermittent character and the small UV fraction of solar light. The association of TiO_2 with an activated carbon (AC) support was proposed as an elegant and appealing solution to offset or cope with these issues [12–15]. In TiO_2-AC composite materials, titania nanoparticles (TiO_2 NPs) are deposited on large surface areas provided by AC, thus allowing easy separation of the composite catalyst from treated water. Within such a composite material both adsorption/desorption and photodegradation mechanisms are expected to occur at the solution/catalyst interface, thanks to the physico-chemical properties of the both components. Moreover, the high sorption capacity of AC enables a possible capture of both initial pollutants and their harmful intermediary products, in particular during sunless periods if solar applications are contemplated. It is also reported that AC in contact with TiO_2 is capable of extending the separation lifetime of photogenerated charges (e^- and h^+) [16, 17], thus increasing the rate of radical generation and improving the photodegradation yield [18, 19]. The synergistic action of both phenomena has then been reported by a number of studies using TiO_2-AC composite materials for pollutant removal in water [20–22]. However, the synergistic effect

targeted in these composite materials do not occurs necessarily in TiO_2-AC but its extent strongly depends on the physical and chemical properties of both TiO_2 and AC, together with the characteristics of their association, the texture, the microstructure and the morphology of the composite material. Furthermore, the strong influence of the synthesis route on the properties of the resulting TiO_2-AC catalyst is most often highlighted. Actually, obtaining a composite material that optimally takes advantage of both sorption and photodegradation capacities, remains a challenging issue. Indeed, there are some risks of obtaining composite materials with substantial degradation of AC porosity [13, 23, 24] and spoilage of TiO_2 photocatalytic properties due to their inaccessibility to light or their structure modification [25]. Typical preparation routes most often reported are sol-gel, hydrothermal and vapor deposition techniques [10, 17, 26]. Sol-gel technique has always been considered as one of the best synthesis route to obtain composite materials with TiO_2 strongly anchored to AC support [13, 27–29]. Unfortunately, this route is tedious most often requiring very strict and controlled condition for the preparation of titania gel. Concerning hydrothermal and vapor deposition techniques, they require respectively vacuum and evaporation reactors likely to increase the cost of the synthesized photocatalyst due to their high energy consumption [13, 30, 31]. On the other hand, one of the simplest ways of taking advantage of both AC adsorption and TiO_2 photodegradation capacities is by simple impregnation of AC with a suspension of preformed TiO_2 NPs [23, 26, 32–34]. However, the weak interactions generated between AC and titania are likely to be broken due to mechanical friction, releasing in the treated solution untied TiO_2 NPs which are hardly discarded from water [17, 26]. Also, the nature of both AC and titania precursors and the ease of the catalyst utilization also determine the attractiveness of a given preparation route. Therefore, the need still arises in developing sustainable preparation techniques which are simple, robust, scalable and cost effective. In a previous work, we have investigated on several ways of associating activated carbon (AC) and titania (TiO_2) into a single material capable of both adsorbing and degrading micropollutants in aqueous solution under UV light [24]. This preliminary study resulted in the development of an attractive synthesis method to prepare cheap and active TiO_2-AC photocatalysts, using a commercial TiO_2 NPs sol for the fixation of titania on a microporous AC derived from shea nut shells (SNS), a typical and abundant tropical biomass residue [24]. The aim of the present work is to demonstrate the

effective and tunable sorption and photo-degradation functionalities of this novel kind of TiO_2-AC catalysts and to elucidate the self-regeneration mechanism of the catalyst. Phenol, a typical refractory aromatic compound considered as a good probe molecule in testing photocatalytic activity for environmental purposes [35, 36], was used in this study.

2. Experimental

Preparation of activated carbon (AC)

AC support is of great importance given that it strongly affects the properties of the TiO_2-AC composite [23, 37]. The homemade AC used in this study was synthesized by a chemical activation method using KOH as the activating agent and shea nut shells (SNS) as the biomass feedstock. SNS were obtained from shea butter production units in Burkina Faso. Annually in Burkina Faso, shea nut processing plants release as by-products up to 40.000 tons of shells [38], which can be used as a cost-free raw material for AC synthesis, given their lignocellulosic nature [39]. The granular size calibrated biomass (0.4 – 2 mm) was impregnated with a 1M KOH solution at a rate of 10 g of biomass for 100 mL of solution, under ambient conditions of temperature and pressure. The paste like biomass recovered after filtration was dried overnight at 105°C in a ventilated oven. The KOH impregnated biomass was carbonized under high purity N_2 flow (Temperature 800°C, heating rate 10°C/min, 150 cm^3/min), in a high temperature programmable rotating furnace (CARBOLITE, MTF Model). The as-obtained carbonized solid was cooled down, grinded and the granulometric fraction under 212 µm was recovered and washed with 1.5 L of distilled water before a final drying step at 105°C overnight. Ultimate and proximate analysis of both AC and SNS (Table S1 in Supplementary Information) has been carried out in compliance with AFNOR standards (XP CEN/TS 14775, XP CEN/TS 15148 and XP CEN/TS 15104).

Preparation of TiO_2-AC catalyst

AC was loaded with titania by a two-step process including an impregnation of the AC support with a commercial titania sol, supplied by *Cristal France SAS, Thann-France*, followed by an annealing step of the TiO_2-impregnated AC in order to anchor the TiO_2 NPs to the carbon matrix. The commercial

titania sol was a stable dispersion of TiO_2 NPs in an acidic aqueous media commonly used as an ingredient for self-cleaning building materials. Typical procedure was carried out as follows. In 50 mL Erlenmeyer flasks containing 10 mL of suspensions of respectively 14.5, 9.7, 4.8 and 1.9 wt% of titania, 1 g of AC was added and the mixture was agitated for 1 hour at ambient temperature. Titania suspensions of different concentrations are prepared by diluting the commercial sol with the appropriate volume of distilled water, pH values varying within the range 2.1-3.2. The solid matter recovered after filtration was dried in an oven at 105°C for 12 h before the final annealing step. The black to brown colored TiO_2-AC composite catalyst (depending on the TiO_2 content) was obtained by heating the sample to 250°C in air (5°C.min^{-1}) followed by the calcination under N_2 flow at 450°C for 2 hours. The sieved fraction of 141±70 µm particle size was recovered and kept in closed plastic containers for adsorption and photocatalytic experiments. For comparative measurements the neat TiO_2 powder has been obtained after drying and calcination at 450°C for 2 hours of the commercial titania sol.

Characterization of AC and TiO_2-AC catalyst samples

AC surface morphology as well as titania particles shape and size were examined by field emission scanning electron microscopy (FESEM, Hitachi S-4800) at 1.5 keV. X-ray energy dispersive spectra were obtained by coupling SEM with a Si (Li) X-ray detector device (BRUKER model, 15 KV). S_{BET} surface areas and pore volume distribution were estimated by N_2 sorption analysis at 77K using Micromeritrics ASAP 2010 equipment (outgassing conditions: 300°C-24h). S_{BET} was assessed with BET (Brunauer-Emmett-Teller) equation applied to the relative pressure between 0.01 and 0.2 where linear transforms and C positive values can be obtained. Mesopores size distribution was estimated by Barrett-Joyner-Halenda (BJH) method applied to the adsorption branch. Crystalline titania phase was analyzed with X-ray diffraction (XRD, PANanalyticalX'Pert PRO) using Ni-filtered Cu-Kα radiation (X-ray power: 40 kV, 20 mA) within the 2θ range 10–100 degree. Thermogravimetric analysis using a Setsys Evolution model was used to determine titania contents of the catalysts [40–43], taking into consideration the ash content of AC component (Table S1 in Supplementary Information). TGA curves of the different samples are provided in Fig. S1 (Supplementary Information). About 5 mg of

size calibrated material (141±70 µm) were used for each test. Later in this document, the TiO_2-AC catalyst with X % titania content is labeled *CATX*. The point of zero charge (pH_{PZC}) of the materials was determined using the mass titration method defined by Noh *et al.* [44]. Boehm's titration with NaOH and HCl was carried out to measure the total amount of basic and acidic sites on the materials surface.

Photocatalytic experiments

Photocatalytic experiments were carried out with phenol solutions prepared from a commercial grade reagent (phenol 99.9 % purity, from Sigma-Aldrich). Adsorption and photodegradation experiments were carried out in magnetically stirred beakers (250 mL) containing 100 mL of the reaction solution (about 30 mm solution height) and the selected catalyst concentration (typically 1 g/L). The light source consists of three neon lamps (VL-320) delivering irradiation with wavelengths ~320 nm and the intensity of 24 W/m^2 at the surface of the treated suspensions. To prevent evaporation, the beakers were covered with UV transparent PMMA (polymethylmetacrylate) lids. At defined time intervals, 2 mL of the suspension were withdrawn and the suspended solid matter removed with a syringe filter (0.45 µm pore size). The residual phenol concentration was determined with a double beam UV spectrophotometer (Shimadzu UV-1601, Japan) at 270 nm wavelength, as reported elsewhere [45–47]. In this study, absorption spectroscopy results were compared to total organic carbon (TOC) in order to assess the level of phenol decomposition and/or mineralization. Comparative adsorption experiments were performed in the same experimental set-up without UV irradiation.

Photodegradation activities were qualitatively assessed by comparing kinetics of phenol degradation over both adsorption and photocatalysis experiments. Kinetics curves were fitted using the exponential model of pseudo-first order kinetics [48]. Catalyst and phenol concentrations as well as light intensity have been kept fixed in all experiments. The study of their influence on the photodegradation rates is beyond the scope of this work. The initial concentration used in this study (100 $g.L^{-1}$) is in the range of the concentrations actually found in a number industrial wastewaters [49]. For adsorption experiments, the amount of phenol ($q_{t,}$ *mg/g*) adsorbed at time ***t*** is calculated according to Equation (1):

$$q_t = \frac{V(C_o - C_t)}{W} \qquad (1)$$

where "C_0" (mg/L) represents the initial phenol concentration, "C_t" (mg/L) the phenol concentrations at time *t*, "*V*" (L) the volume of the suspension, "*W*" (g) the mass of the catalyst.

Phenol adsorption isotherms of AC-TiO_2 catalysts and uncoated AC were obtained by varying their concentrations within the range 0.1 – 8 g/L while keeping constant the initial pollutant concentration (100 mg/L). The standard errors were estimated lower than 5% on kinetics measurements carried out in this study.

3. Results and discussion

TiO_2-AC catalyst surface morphology

SEM micrographs of TiO_2-AC catalysts (Fig. S2a in Supplementary Information) exhibit a macroporous texture which could be assigned both to the high production of gas during KOH activation process and the structure of the starting biomass precursor [35, 50, 51]. The size of the opened macropores are estimated in the range from hundreds nm to few µm. Actually, in addition to their facilitating role in the migration of pollutant molecules from the bulk toward the internal microporosity, the external macropores of the carbonaceous support is favorable to optimal photoactivation of embedded TiO_2 NPs which could be easily irradiated. Indeed, a number of macropores occupied by small aggregates of TiO_2 NPs are shown in Fig. S2b-c (Supplementary Information). The TiO_2 NPs size estimated on micrograph pictures range from 20 to 40 nm, which is in the range of size provided by the titania sol provider (Table 1). Despite the presence of few aggregates, the regular deposition of nanoparticles observed on SEM images suggests that the coating process allowed TiO_2 NPs to well disperse over AC support. The latter provides a large surface area for titania regular deposition within macropores. From the SEM images, it can be noticed that the density of TiO_2 NPs on the surface of TiO_2-AC catalysts seems to increase gradually with the titania content (Fig. S2c-e in Supplementary Information). Moreover, the increasingly closer arrangement of the TiO_2 NPs at higher titania content on AC support seems to generate additional porosity whose size

is of the same order of magnitude of the TiO_2 NPs (Fig. S2c and S2d in Supplementary Information). The occurrence of additional porosity on TiO_2-AC catalysts will be further discussed later in this document, regarding the porous texture characterization.

Table 1 Physico-chemical parameters of AC, neat TiO_2 nanoparticles and different *CATX* catalysts

Sample	TiO_2 (% wt)	S_{BET} ($m^2.g^{-1}$)	Crystallite size of anatase phase (nm)	Particle size (nm)	V_{total} ($cm^3.g^{-1}$)	$V_{microporous}$ ($cm^3.g^{-1}$)	pH_{pzc}	Acidic group (mmol.g^{-1})	Basic groups (mmol.g^{-1})
CA	0	571	/	/	0.272	0.252	9.2	0.303	0.552
CAT34	34	602	16.1	~20-40	0.286	0.257	4.2	0.541	0.241
CAT25	25	609	15.9	~20-40	0.285	0.248	4.1	0.532	0.251
CAT14	14	631	12.1	~20-40	0.298	0.253	4.8	0.523	0.249
CAT11	11	625	12.2	~20-40	0.326	0.250	4.9	0.525	0.256
Neat TiO_2	100	98	15.2	20-30[a]	/	/	3.8	/	/

[a] Data provided by the supplier.

The presence of titania were also detected by EDX analysis (Fig. S3 in Supplementary Information). In the case of CAT34 and CAT25 catalytic material, titanium represents 38 and 21 wt% of the total chemical elements at the surface of the catalyst. Assuming that all titanium is in titania phase, the corresponding TiO_2 content is estimated (from atomic ratio) to reach ~ 63 and 35 wt%. These values can be considered as an average on the catalyst surface given the regular deposition of titania. Given the average values of titania contents determined by TGA method (34 and 25 wt%), it can be concluded that TiO_2 NPs are mainly concentrated at the surface of the catalyst. This result is of a high benefit for photocatalytic reactions, as only the TiO_2 NPs at the superficial part of the catalyst are more accessible to UV light irradiation.

Apart from carbon (C) and oxygen (O) which are common elements, potassium (K) and silicium (Si) were also detected (Fig. S3 in Supplementary Information). K element could be the residuals of activating KOH used during AC synthesis while Si element might originate from the SNS biomass raw material.

Characterization of crystalline TiO_2 phase

XRD patterns of AC, neat TiO_2 and different TiO_2-AC catalysts are depicted in Fig. 1. On TiO_2-AC diffractograms, the presence of anatase phase (JCPDS Card no. 21-1272) is evidenced by peaks at 2θ values of 25.3°, 37.8°, 48.0°, 53.8°, 54.9° and 63°, corresponding to (101), (004), (200), (105), (211) and (204) crystal planes [52]. Virtually no presence of rutile phase has been detected by XRD analysis. The anatase phase initially found in the pristine sol (Fig. 1), is still present in the catalysts to ensure their photoactivity. By contrast, the XRD pattern of neat TiO_2 submitted to an annealing treatment at 450°C (Fig. 1) reveals the appearance of peaks corresponding to crystal planes of (110), (101), (200), (111), (210), (211), (220), (002) and (310) of the rutile phase (JCPDS Card no. 21-1276). This feature suggests that the anatase phase transformation to rutile is complete after the annealing treatment at 450 °C for the neat TiO_2 sample and clearly demonstrates the stabilizing effect of AC support against anatase phase transformation into rutile, known to possibly start from 400°C [13, 53, 54]. This stabilizing effect, assigned to the interfacial energy between AC and titania [13, 28, 32], is of particular interest for the photocatalytic performances of the composite material as it enables the maintain of photocatalytic activity of anatase nanophases while ensuring a good anchorage between AC and TiO_2 NPs through the annealing treatement. This strong anchorage of TiO_2 NPs on the AC is supported by the fact that less than 6 wt% of titania were lost when the catalyst is recovered after stirring during 5 h in aqueous solution. Titania loss was determined by the difference of the titania contents measured from TGA method before and after the aforementioned mechanical stability test. Such a strong interaction was likely favored by the annealing treatment as reported elsewhere [12, 13, 16, 55].

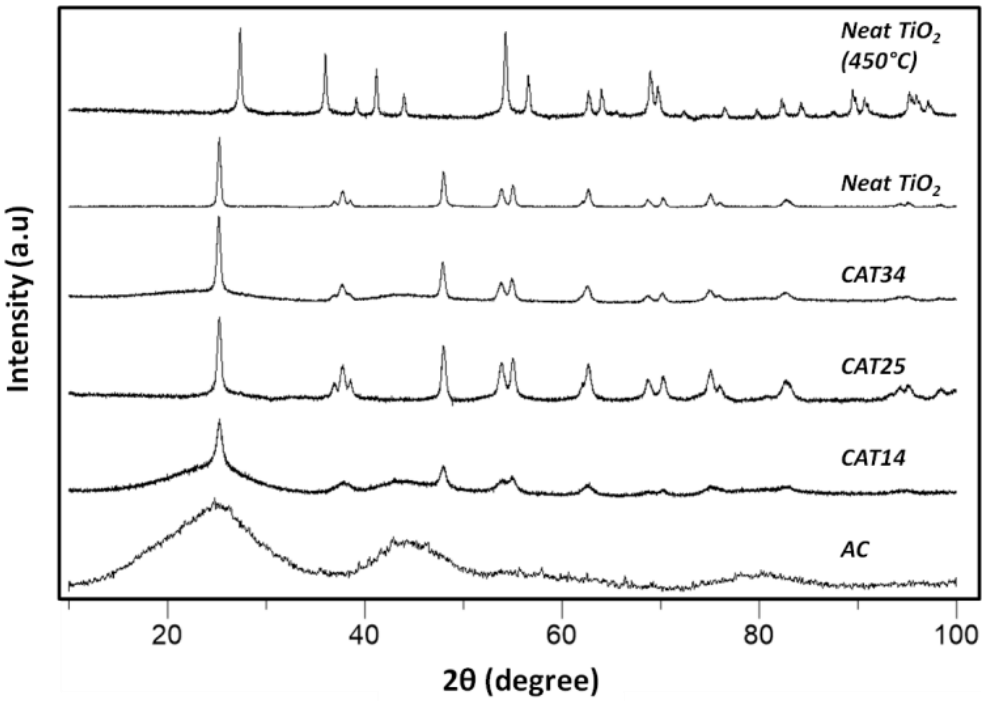

Fig. 1 XRD patterns of AC, neat TiO_2 nanoparticles and *CATX* catalysts, obtained with different *X* % wt/wt titania

From the XRD patterns, the mean size of anatase crystallites *(D)* was estimated by Scherrer's formula applied to the (101) diffraction peak, assuming spherical crystallites. Considering the nanoparticle average sizes approximated from SEM images (20-40 nm), the XRD analysis suggests that TiO_2 NPs are in the form of small aggregates of anatase crystallites. The size and microstructure of TiO_2 NPs are important parameters for photocatalysis efficiency since they influence the electron/hole charges recombination and the available photoactive surfaces necessary for UV light harnessing [56]. The estimated particle sizes obtained in this study are in the range of the optimal particle size generally reported in the literature [56, 57] which is close to the particle size of commercial P25 titania (20 nm). On XRD pattern of AC (Fig. 1), no characteristic peaks have been observed, suggesting the amorphous state of the carbonaceous support.

Porous textural properties of the TiO_2-AC catalysts

N_2 adsorption-desorption isotherms for the uncoated AC and the TiO_2-AC catalysts are depicted in Fig. 2a. AC reveals a typical type I isotherm, evidencing the prevalence of micropores [26]. On the other hand, TiO_2-AC catalysts (*CAT 11*, *CAT14*, *CAT25* and *CAT34*) set out composite isotherms of type I and IV, characterizing the presence of mesopores. It is worth mentioning that the TiO_2 NPs coating treatment has modified the porosity of the catalyst without causing any reduction of the AC specific area as detailed in Table 1. Interestingly, the BET specific areas for all the TiO_2-AC catalysts has slightly increased and could be assigned to which could be associated with the formation of additional mesopores on the AC surface. This phenomenon could arise from the close arrangement of the TiO_2 NPs on the AC surface. Indeed, it can be observed in Fig. 2b that the size of generated mesopores is influenced by the titania content in the TiO_2-AC catalyst. The lower size of mesopores observed on *CAT34* can be explained by the closer arrangement of the TiO_2 NPs due to the higher titania loading and is consistent with the occurrence of TiO_2-constituted mesopores walls. The fact that BET specific area reaches a maximum for *CAT14* suggests that increasing the TiOs NPs content in the TiO_2-AC above an optimum value leads to some clogging of the pores initially crated by the close arrangement of the TiO_2 NPs on the AC surface. Another possible explanation of this porous textural modification is the effect of the annealing thermal treatment creating new type of carbon pores of larger sizes. In this case, the additional porosity could also be the result of carbon partial oxidation reactions occurring during the annealing step [58]. Indeed, the acidity of the impregnating TiO_2 NPs suspension (ranging from 2.1 to 3.2) has acidified AC surfaces as suggests by the zero point of charge values (pH_{zpc}) which shifted from basic pH value on uncoated AC to acidic pH value on TiO_2-AC catalysts (Table 1). These acidic oxygenate functions could play the role of oxidant during the annealing thermal treatment resulting in an increase of the AC porosity.

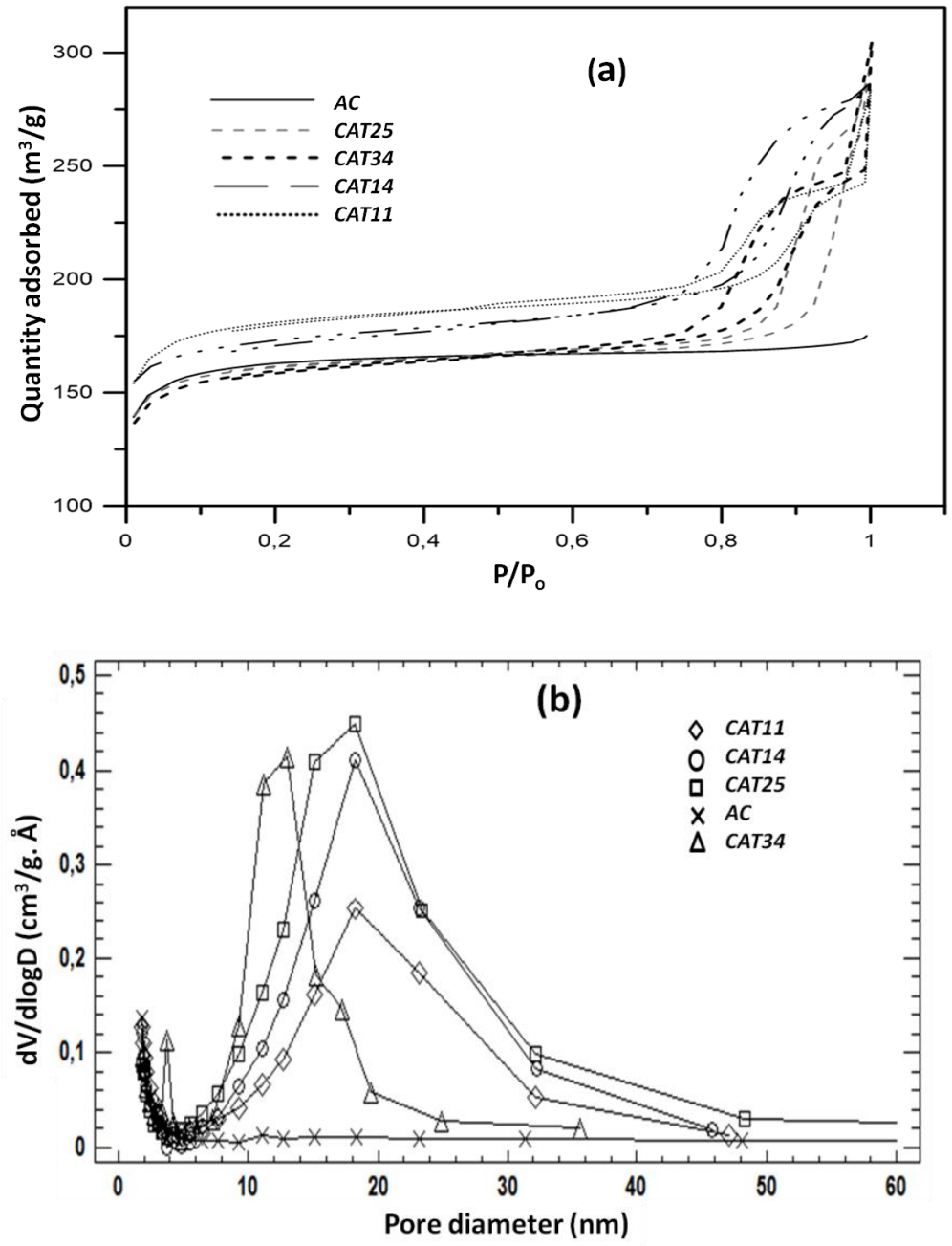

Fig. 2 (a) N_2 adsorption desorption isotherms, (b) Pore size distribution of uncoated AC and *CATX* catalysts

As far as literature is concerned, preparation of supported titania on AC matrix has most often been associated with the reduction of the TiO_2-AC surface area, as compared to the uncoated AC [13, 23, 32]. In this study, the surface area was not altered and virtually zero variation of micropore volumes was observed (Table 1). Indeed, the use of preformed TiO_2 NPs (20 – 40 nm) in aqueous media prevents titania to enter the narrow porosity. As mentioned earlier, titania is preferentially located

within opened and light exposed large pores, as opposed to other synthesis routes likely to favor the formation of nanoparticles within the internal porosity of the catalyst [13, 23, 32]. Furthermore, the occurrence of additional mesopores in the catalyst, due to their low potential energy escape surfaces, is of interest to favor internal diffusion mass transfer during photocatalytic reactions and thus improve the degradation kinetics.

Adsorption properties of the TiO_2-AC catalysts

The adsorption capacities of both TiO_2-AC composites and uncoated AC were assessed through phenol removal in aqueous solution. The equilibrium of phenol adsorption in aqueous solution was virtually reached within 1h contact time in the absence of UV light and the corresponding adsorption isotherms are depicted in Fig. 3a. Langmuir and Freundlich adsorption isotherm models, the most widely reported in the literature, have been used and the related adsorption parameters are presented in Table 2. The phenol adsorption capacities obtained are in line with the performances of AC adsorbents obtained by other authors from tropical biomasses [60, 61]. The improvement of adsorption capacity on CAT25, CAT14 and CAT11 over the initial uncoated AC can be explained by a slight increase of the specific surface area discussed earlier. Moreover, parameter values from Langmuir and Freundlich models of phenol adsorption (Table 2) suggest that phenol adsorption capacity of the catalyst follows a general downwards trend with an increase of their titania content. This finding can be explained by the hindrance of AC adsorption sites by TiO_2 NPs. In addition, the fact that neat titania adsorbs less than 3 % of phenol (results not shown) confirms that its presence may not play a significant role in the adsorption capacity of the composite catalyst. In the literature, two main adsorption pathways of phenol on AC are typically reported [35, 37, 59] : (i) physical adsorption as a result of dispersive interactions between the aromatic phenol and AC carbon basal planes and (ii) the chemisorption through ester and/or phenoxo bond formation between the OH groups of phenol and the carboxylic groups, if any, onto AC surfaces. In addition, in aqueous solution, the oxygenated groups on the titania surface can react with phenol to form phenoxo bonds. The extent of this form of adsorption on TiO_2-AC catalysts seems to be very low given the negligible quantity of phenol adsorbed by neat titania.

The extent of physical adsorption versus chemical adsorption phenomena in the mechanisms of phenol adsorption over the different materials can be appreciated by studying the electrostatic effects on the phenol adsorption taking into account the pH values of the solutions and the pH_{zpc} values of the materials. Indeed, depending on both the pH of the solution and the pH_{zpc} of the materials, the surface functional groups may exhibit positive or negative charges and exert an electrostatic attractive or repulsive force towards phenol. The difference in pH_{zpc} between AC and TiO_2-AC catalysts is consistent with the density of basic and acidic groups found on the different materials (Table 1). The high density of basic groups on uncoated AC then corroborates with its basic pH_{zpc} value (9.2) and resulted from the KOH activation during AC preparation. In TiO_2-AC catalysts, these basic groups have been neutralized by the high acidity of the sol used to load TiO_2 NPs, leading to lower pH_{pzc} values on the composite materials. During phenol adsorption experiment with the different materials, solution pH was not adjusted and was initially close to 6. In these conditions, only AC exhibits a surface charge globally positive ($pH< pH_{zpc}$) while TiO_2-AC catalysts exhibit a surface charge globally negative ($pH>pH_{zpc}$). Moreover, in all cases, phenol was present in his acid form (pKa =9.9) and any electrostatic effect was thereby limited. On the other hand, a pH decrease at phenol adsorption equilibrium was observed in all case suggesting that phenol has reacted with some basic functional groups of the materials (Table 1) leading to phenolate ions in attractive electrostatic interactions with AC but in repulsive electrostatic interactions with TiO_2-AC catalysts. By considering the phenol adsorption capacities of the different materials (Table 2 and Fig. 3), it can be concluded pH-dependant chemical adsorption phenomena were not predominant in the mechanism adsorption of phenol in these conditions, as reported elsewhere [49]. Actually, the higher adsorption capacities presented by the composite materials sustain that the phenol is mainly adsorbed through Van der Waals-type physical interactions between the aromatic rings of the phenol molecules and the aromatic rings of CA involving π electrons. These non-specific physical interactions are likely to be enhanced by the porosity of the materials. Therefore, the porosity modification observed after titania coating process better explains the adsorption improvement on the composite materials. This interpretation is also supported by the fact that the best fitting for the experimentally measured adsorption isotherms has been obtained with the Langmuir model, indicating a significant homogeneity of the adsorption sites

on the adsorbent surface [60, 61]. Such homogeneous adsorption surface of the catalyst might be assigned to the high density of π electrons adsorption centers. It is worth mentioning that this kind of weak physical interactions between pollutant and the TiO_2-AC catalyst is of particular interest for their degradation performances insofar the pollutant adsorbed in weak interaction with the AC would easily be desorbed and migrate toward photoactive TiO_2 centers to undergo photodegradation [62].

Assuming that phenol is adsorbed only on the AC component of the catalysts, the adsorption capacities have been normalized to the AC content in the solution. The normalized isotherms (Fig. 3b) were obtained from pristine isotherms (Fig. 3a) by dividing the phenol equilibrium adsorbed amount q_e by the AC content of the different materials. Regardless to the experimental and calculation errors, the slight dispersion of the adsorption equilibrium points on normalized isotherms could be attributed to the limited influence of titania content on the adsorption capacity of the AC support. This finding suggests that for a catalyst with a given titania content, the adsorption capacity is only related to the total amount of AC and it does not change as a function of titania loading. Interestingly, this finding suggests the fact that with the protocol used in this study, it is possible to play on titania content parameter to provide a given catalyst with the desired adsorption capacity. On the other hand, the position of the normalized isotherms of TiO_2-AC in comparison with uncoated AC isotherm (Fig. 3b) highlights the slight increase of the AC adsorption capacity after the titania coating process.

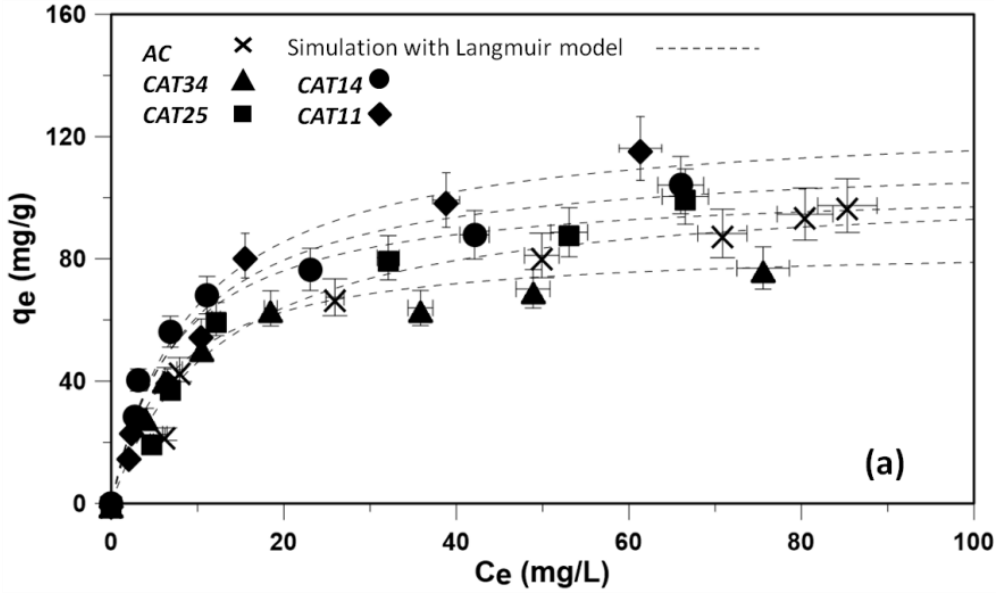

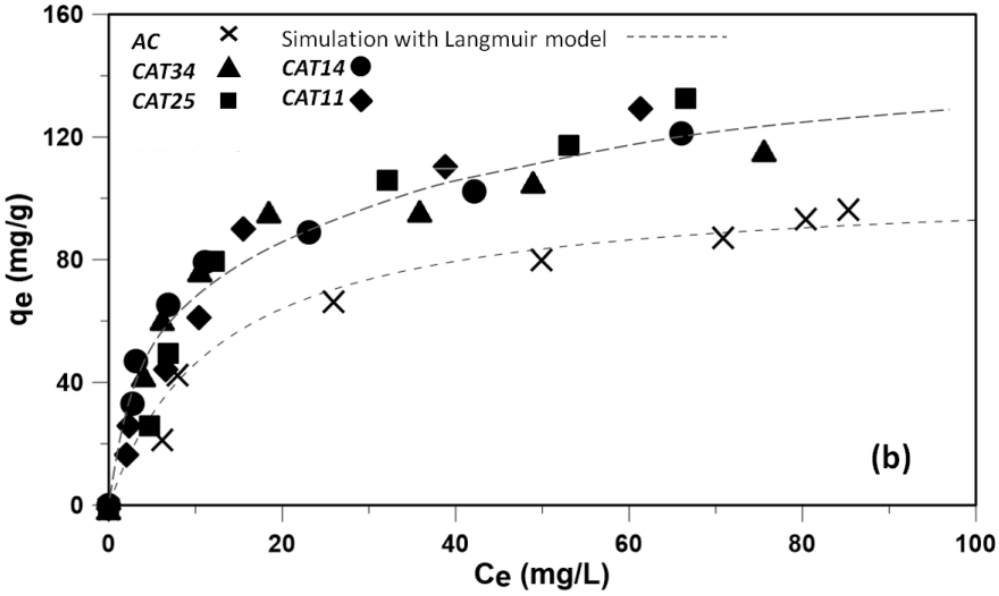

Fig. 3 (a) Phenol adsorption isotherms of AC and *CATX* catalysts measured at 298 K, (b) After a normalization treatment according to the AC content

Table 2 Parameters of Langmuir and Freundlich models of phenol adsorption

Catalyst	*Langmuir model parameters* $q_e = \frac{q_{max} \cdot b \cdot C_e}{1 + b \cdot C_e}$					*Freundlich model parameters* $q_e = K_F \cdot C_e^{\frac{1}{n}}$				
	q_{max} (mg.g^{-1})		b (L.mg^{-1})		R^2	k_F (mg.g^{-1})(L.mg^{-1})$^{1/n}$		n		R^2
	Value	S.E.[a]	Value	S.E.[a]		Value	S.E.[a]	Value	S.E.[a]	
AC	117,4	6,5	0,0497	0,0082	0,9849	13,2	3,3	2,18	0,33	0,8967
CAT34	82,3	2,5	0,1414	0,0235	0,9953	22,5	3,3	3,31	0,52	0,8904
CAT25	124,5	9,9	0,0558	0,0103	0,9756	12,3	3,6	1,92	0,35	0,8856
CAT14	111,5	5,1	0,1303	0,0253	0,9895	25,2	3,3	2,85	0,38	0,9167
CAT11	142,4	6,8	0,0676	0,0070	0,9888	13,5	2,1	1,78	0,19	0,9464

[a] Standard error for the determined paramater

Photocatalytic activities of the TiO_2-AC catalysts

Both kinetics of phenol photocatalytic degradation and removal by simple adsorption into the TiO_2-AC catalysts have been studied (Fig. 4). Blind experiments without the catalyst confirmed that a negligible quantity of phenol (2.5%) is removed over 10 hours UV irradiation duration. As expected, phenol photolysis is negligible. Thus, whatever the physico-chemical mechanisms involved, the

phenol removal in the liquid phase is assigned to the presence of the TiO_2-AC catalyst. All the TiO_2-AC catalysts reveal a behavior similar to that detailed in Fig. 4 for *CAT25* which exhibits the best degradation performances. In the absence of UV irradiation, the phenol concentration drops abruptly in the early moments of the experiment followed by an asymptotic evolution until the achievement of equilibrium obtained in less than one hour, corresponding to the phenol adsorption over the catalyst. The rate of phenol adsorption that quickly changes during this period is mainly controlled by mass transfer phenomenon inside the microporous network of the activated carbon. Phenol concentration remains perfectly stable once the conditions of equilibrium between adsorbed phase phenol and bulk phase phenol are reached. The contribution of the photocatalyst is demonstrated by the direct comparison of the kinetic curves obtained in absence and in presence of UV irradiation. In this latter case, TiO_2 nanoparticles mainly present at the activated carbon surface are submitted to the UV irradiation and therefore photo-activated. The initial phase of rapid decay of phenol concentration is little changed. This clearly indicates the prevalence of adsorption phenomena over photodegradation reactions, in terms of kinetics. However in the presence of UV irradiation, phenol degradation by free radicals attacks over photoactive titania centers prevents the equilibrium achievement inside the reactive system. This degradation leads to a slower but continuous decrease of phenol concentration in the liquid phase until virtually complete removal of phenol from the treated solution after 10 h of UV irradiation (Fig. 4). This behavior was obtained with all the TiO_2-AC catalysts and demonstrates the occurrence of the two functionalities targeted for the catalysts, i.e. adsorption and degradation/mineralization of the pollutant.

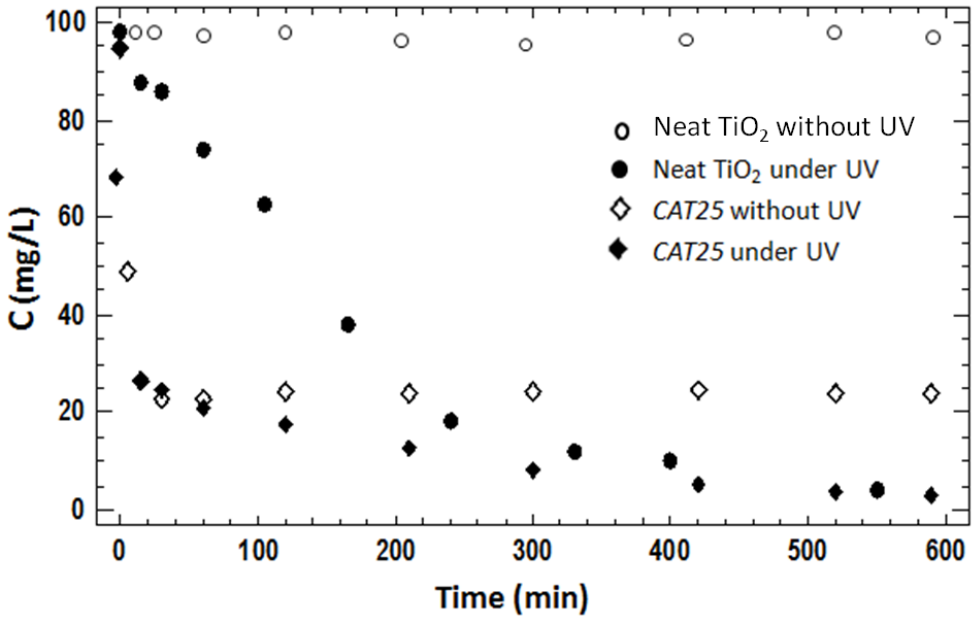

Fig. 4 Kinetics of phenol abatement through adsorption and photocatalytic degradation on neat titania and *CAT25*, the composite catalyst with 25% wt/wt titania ratio)

The high initial rate of phenol removal suggests a high adsorption capacity of the catalyst which concentrates the phenol molecules within its internal porosity during the first hour of the reaction. For the sake of comparison the catalytic activity of neat titania is also presented in Fig. 4. While up to 70% of phenol is removed after 1h from the solution containing *CAT25* catalyst, only ~20% is eliminated by the effect of neat TiO_2 NPs within the same time. The low adsorption capacity of titania then prevents the phenol to concentrate around the photocatalytic centers of the catalyst. These results confirm the synergistic effect of adsorption and photocatalysis on TiO_2-AC composite materials as reported elsewhere [12, 13, 23, 28, 63, 64]. Interestingly, the improvement of the catalyst adsorption capacity observed in this study after titania coating has never been reported in the literature yet.

Fig. S4 (Supplementary Information) presents the variation of TOC as a function of phenol concentration determined during photocatalysis experiments. Regardless the material used (uncoated AC, neat titania or AC-TiO_2 composite material), the plots of TOC as a function of phenol concentration always describe a linear trend near the theoretical line of TOC calculated from the

corresponding phenol concentration suggesting that there are no detectable organic compounds (e.g. degradation products of phenol) other than phenol in the liquid phase.

Therefore, the photodegradation of phenol in the treated solution seems to reach almost total mineralization of the pollutant in the liquid phase with negligible quantities of intermediary products. This corroborates with the typical shape of phenol UV-visible absorption spectrum of the solution (not shown) which doesn't change whatever the concentration during the experiments. According to the literature [17, 23, 65], the limitation of degradation intermediary products as reported in this study is correlated with the efficiency of the photocatalytic system. Benzoquinone, hydroquinone and catechol and a number of short chains aliphatics are intermediary products generally detected in TiO_2-AC photocatalytic systems [66]. Interestingly, their production seems to be very limited in this study.

The photocatalytic degradation was further tested with the TiO_2-AC catalysts containing different amount of titania. Starting from initial phenol concentrations of 100 mg/L, the residual concentrations after one hour during which mainly phenol adsorption occurs were 26, 18, 14 and 11 mg/L, respectively for the catalysts *CAT34*, *CAT25*, *CAT14* and *CAT11*. Fig. 5 depicts the kinetics of phenol removal for the different TiO_2-AC catalysts after this first adsorption phase, during which the kinetics of phenol removal is mostly driven by the photocatalytic effect of the TiO_2-AC composites.

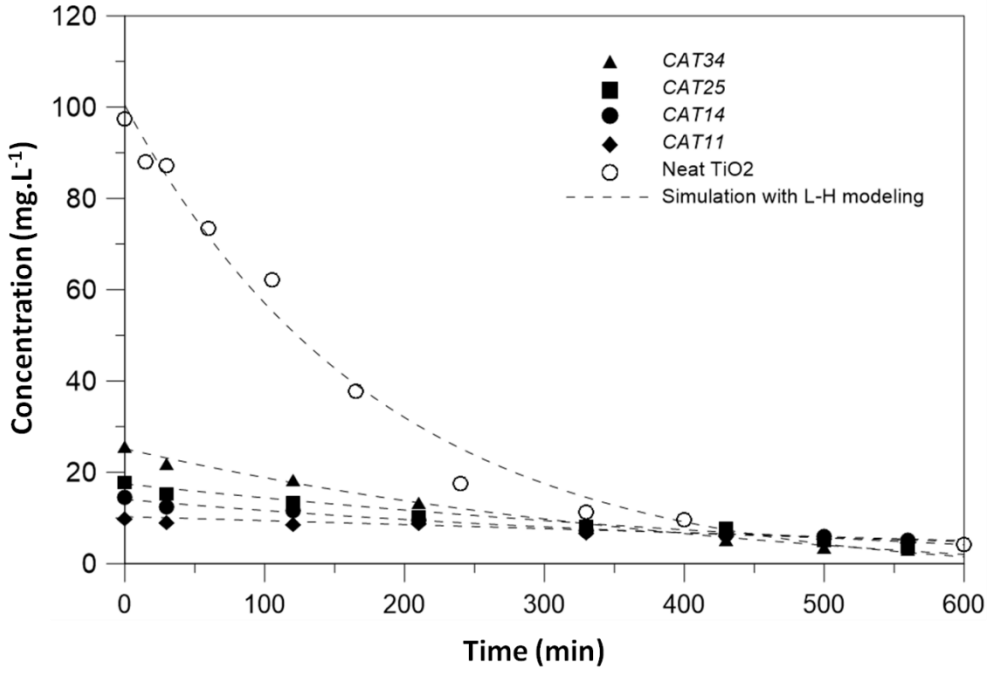

Fig. 5 Photocatalytic kinetics of phenol removal with *CATX* catalysts and neat TiO_2 The zero time in this figure correspond to t = 1h in the whole experiment

Kinetics of photocatalytic removal of phenol

Removal of pollutant from solutions through heterogeneous photocatalysis is commonly described with the Langmuir-Hinshelwood kinetic model [15, 67], expressed in Equation (2) where k ($L.mg^{-1}$) denotes the reaction rate constant and K ($mg.L^{-1}.min^{-1}$) the adsorption coefficient.

$$\frac{dC}{dt} = -k\frac{KC}{1+KC} \quad (2)$$

Equation (2) is most often simplified into pseudo first order equation for low pollutant concentrations ($< 10^{-3}$ $mol.L^{-1}$)[67]. The expression of concentration is then given by Equation (3), with k_{app} (min^{-1}) denoting the apparent pseudo first order constant.

$$C = C_0 e^{-k_{app}t} \quad (3)$$

Different k_{app} values were obtained with catalysts of different TiO_2 amount (Table 3), after calculation fitting with experimental data (Fig. 5).

Table 3 Apparent pseudo first order kinetic constants obtained for neat TiO_2 nanoparticles and different *CATX* catalysts

Sample	*CAT34*	*CAT25*	*CAT14*	*CAT11*	Neat TiO_2
Adsorption equilibrium concentration (C_0, $mg.L^{-1}$)	26	18	14	11	97
k_{app} (10^{-3} min^{-1})	3.64	2.36	1.90	1.10	5.55
Standard error (10^{-3} min^{-1})	0.09	0.12	0.05	0.06	0.22
R^2	0.99	0.95	0.98	0.94	0.97
Normalized k_{app} (10^{-3} min^{-1})	10.7	9.44	13.6	10.0	5.55

The value of R^2>0.95 (Table 3) actually indicates that phenol removal after the initial one hour-adsorption phase can be efficiently described by first order kinetic model. The value of k_{app} increases with the titania content of the catalyst. This interesting feature translates an effective photocatalytic

effect of the TiO_2 NPs and indicates that the pollutant degradation functionality in the TiO_2-AC catalyst prepared in this work can be advantageously tunable by varying the TiO_2 content in the composite material, probably thank to both the favorable location and dispersion of the TiO_2 NPs into the carbon matrix, as demonstrated previously.

On the other hand, it is worth mentioning that at t = 0 (which corresponds to t=1 h considering the whole experiment), the TiO_2-AC catalysts have already adsorbed the major part of pollutant initially present in the solution (100 $mg.L^{-1}$). At the end of the experiment the same removal level is reached with both neat TiO_2 and the composite materials suggesting similar overall removal efficiencies but with significantly different adsorption/photodegradation contribution. Given that k_{app} only concerns pollutant removal in the solution but not on the catalyst and considering the pollutant adsorption equilibrium reached at t=0, removal of pollutant from the solution is undoubtly associated with the photodegradation of the pre-adsorbed molecules on the catalyst, through continuous equilibrium displacement of pollutant concentration between adsorbed and liquid phases. This fact will be confirmed and thoroughly discussed later in the next section (Catalyst recycling).

k_{app} value of neat TiO_2 NPs ($5.55\ \ 10^{-3}$ min^{-1}) is higher compared to the values obtained with the TiO_2-AC catalysts (Table 3). This single parameter should be used to compare the photocatalytic efficiency of the materials while keeping in mind that (i) the TiO_2 content are not the same, and (ii) the phenol adsorption/photodegradation contribution in the overall mechanism of phenol removal is also different in the materials. Indeed, phenol being degraded by neat TiO_2 NPs comes directly from solution (very low amount adsorbed) while on the composite catalyst, photodegradation activity concerns both the molecules coming from the solution and the pre-adsorbed molecules coming from the catalyst internal porosity. The interest of the TiO_2-AC catalysts towards the neat TiO_2 NPs is clearly highlighted while considering the amount of TiO_2 used in the catalysts. Few amounts of TiO_2 are used on the composite materials to obtain the same level of removal as obtained with the use of up to ten times more amount of neat TiO_2. Assuming that kinetic rate is proportional to titania content in first approximation, k_{app} can be normalized to the amount of TiO_2 for all the composite materials and the neat TiO_2 NPs (Table 3). The normalized k_{app} values of the composite materials are higher than that of neat TiO_2 NPs,

suggesting that TiO_2 NPs are better exploited for photocatalytic reactions in TiO_2-AC catalysts than in neat TiO_2 NPs. The high benefit of concentrating the pollutant within the AC internal porosity close to TiO_2 NP_S is thereby demonstrated, in accordance with previous work [17, 52]. However, here interestingly, the *CAT14* catalyst exhibits a higher normalized k_{app} value than those obtained with *CAT34*, *CAT25* and *CAT11*. This finding suggests that for this family of composite materials, an optimum TiO_2 content leads to the best exploitation of photocatalytic activity of TiO_2 and to an optimum synergistic effect between adsorption and photodegradation phenomena. This optimum TiO_2 content has to be correlated to both the textural and microstructural features of the TiO_2-AC nanocomposite materials previously described. When TiO_2 content increases in the composite materials, the number of photoactive sites increases provided that the TiO_2 anatase crystallite are exposed at surface particle and reached by the UV radiation.

From a general performance point of view, the phenol removal rate found in this study is in line with those typically reported in the literature [12, 68]. However in this work, it is demonstrated that the studied TiO_2-AC composite catalyst could overpass the previously reported systems most often requiring much higher amount of photocatalytic materials for the same level of pollutant elimination. Furthermore, the activity of the catalysts studied in this work was assessed with a UV light source providing an intensity of about 24 W/m^2, which is lower compared to solar UV light, sometimes registered in sunny areas of subsaharian African countries. In these areas where UV irradiation peaks easily cap 70 W/m^2, higher performances of the studied catalytic systems are expected in terms of photodegradation kinetics. Indeed, in a previous paper our research team highlighted that photodegradation activity is proportional to UV light intensity [69].

Catalyst recycling

As mentioned in the introduction, the challenge of TiO_2-AC composite materials is to combine sorption and mineralization of pollutant as efficiently as possible. This double functionality is of interest only if pollutant degradation due to the photocatalyst is not limited to the liquid phase but allow total or partial pollutant desorption within the AC microtexture. This condition is a prerequisite for (i) an effective coupling between the both physico-chemical processes and (ii) an actual interest for

a solar photocatalysis application. This property is actually evidenced by the several successive treatment cycles of phenol by the same TiO_2-AC catalyst (*CAT25*) depicted in Fig. 6. At the end of each treatment cycle of 24 hours duration under UV irradiation, the solution is concentrated in phenol in order to start a second treatment cycle from an initial phenol concentration of 100 $mg.L^{-1}$. This operation is performed with the TiO_2-AC catalyst (*CAT25*) or the uncoated AC. For the uncoated AC, it is observed an almost complete saturation of the adsorbent after the third treatment cycle. Only 9 wt% of phenol present in the solution is adsorbed during the third cycle. Contrastingly, with the presence of photocatalyst, the TiO_2-AC composite material keeps interesting adsorbing properties depicted by the initial phenol concentration drop at the beginning of each treatment cycle which actually occurs even during the third cycle although in a lesser extent. This ability of the composite material to adsorb phenol over several and successive cycles (without any regeneration treatment), together with the comparison of the phenol concentration profiles obtained with uncoated AC, are the experimental demonstration of the occurrence of both desorption and degradation/mineralization of phenol and derived products that actually occurs at the surface of the composite material probably within the mesoporous network of the TiO_2 NPs. Under UV irradiation, the photo-induced radical reactions generated within the porous TiO_2-AC network allow a self-generation of the activated carbon whose extent especially depends on irradiation conditions, irradiation duration, and initial loading level of activated carbon.

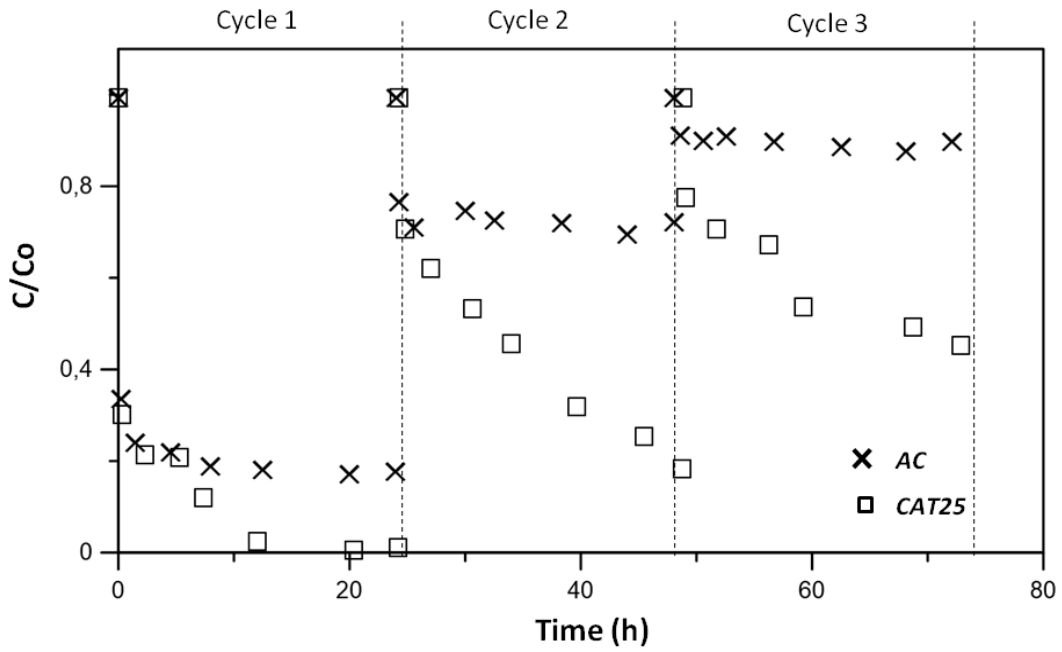

Fig. 6 Kinetics of the phenol removal on *CAT25* and uncoated AC catalyst over 3 consecutive cycles **(**C_o= 100 mg/L, adsorbent concentration= 1g/L)

Moreover, the virtually preserved photoactivity over several cycles indicates that titania is strongly anchored to the AC support. The proposed coating route enables a good anchorage of titania on the carbon matrix as discussed previously. However, few titania amount losses (6% registered after the first cycle) could explain partly the slight decrease of removal efficiency over the following cycles. Further investigations on the influence of the annealing treatment conditions are in progress in order to further strengthen the TiO_2-AC anchorage and improve the catalyst stability.

As far as reaction mechanisms are concerned, it is reported that the photodegradation rate is generally limited by mass transfer phenomena [23, 52, 69]. The transfer phenomena involve the transfer of the pollutant from the bulk solution to the catalyst and afterward, from their adsorbed location to the photoactive centers on the catalyst. The high adsorption capacity of TiO_2-AC catalyst is then important to reduce the rate limiting transfer step from the bulk to the catalyst. Given its molecular size a pollutant like phenol is known to be adsorbed mainly within the micropores. TiO_2 NPs were found to be located at the external macropores and to be associated with the formation of additional mesopores. A number of degradation mechanisms proposed in the literature [12, 52] have most often been

illustrated as the synergistic effect of photoactive titania particles in close contact with AC, but few of them emphasizes on the location differences of pollutant and TiO_2 NPs on the composite catalyst.

Based on the results obtained in this work, we were able to propose a mechanism on the coupling of adsorption and photocatalytic degradation of phenol taking into account both the physico-chemical features of the prepared TiO_2-AC materials and the different kinetic profiles of pollutant removal in the liquid phase (Fig. 7).

The photochemical mineralization of phenol molecule through formation of free radicals and intermediary products is well documented [66, 70] and is not taken into consideration in the proposed mechanism. In the earlier moments of the experiment, the high concentration gradient between the bulk solution and the adsorbent (Fig. 7B) is responsible of the rapid migration of the pollutant from the bulk to the internal porosity of the catalyst (Fig. 7C). Considering the very high adsorption rate at this stage, the pollutant diffuses very rapidly through TiO_2 NPs located on the external macropores, without being immediately photodegraded. Afterward, the adsorption rate decreases progressively until getting negligible when pseudo equilibrium between the adsorbed amount of the pollutant and the corresponding concentration in the bulk is obtained (Fig. 7D). At this moment, the effect of photodegradation actually becomes perceptible and proceeds at the catalyst surface UV irradiated titania. The pseudo equilibrium is then shifted, inducing a further transfer of pollutant from the bulk to the surface of the catalyst, as well as from the internal porosity to the external irradiated mesoporous and macroporous TiO_2-AC network (Fig. 7E). The occurrence of external mesopores associated with the presence of TiO_2 NPs is expected to play an important role in this diffusion mass transfer mechanisms along with the efficiency of the coupling of adsorption/desorption phenomena and photocatalytic reactions.

Pollutant being degraded coming simultaneously from the solution and the catalyst itself, and the decrease of pollutant occurring in both phases (Fig. 7F). The proposed photocatalytic pathway suggests that the pollutant removal from water takes place while the catalyst itself is freed of the pollutant. It also highlights the “self-regeneration” capacity of the catalyst which enables the preservation of the performances and stability over several cycles. However as mentioned with Fig. 6, the performances of the catalyst slightly decrease on the second and third cycle. This can be explained

by the fact that after the first cycle, a residual amount of adsorbed pollutant remains adsorbed and is difficult to discard from the catalyst (Fig. 7F). This residual concentration is either irreversible [71] or needs longer time for complete diffusion of the pollutant from the adsorption site toward the photoactive centers, then allowing the catalyst to be completely refreshed (Fig. 7G). To the kinetics of pollutant removal experimentally obtained can be affected numerical coefficients which are determined by mathematical modeling of pollutant mass balance around the photocatalytic system. This aspect of the study is under consideration and will be presented in an upcoming paper.

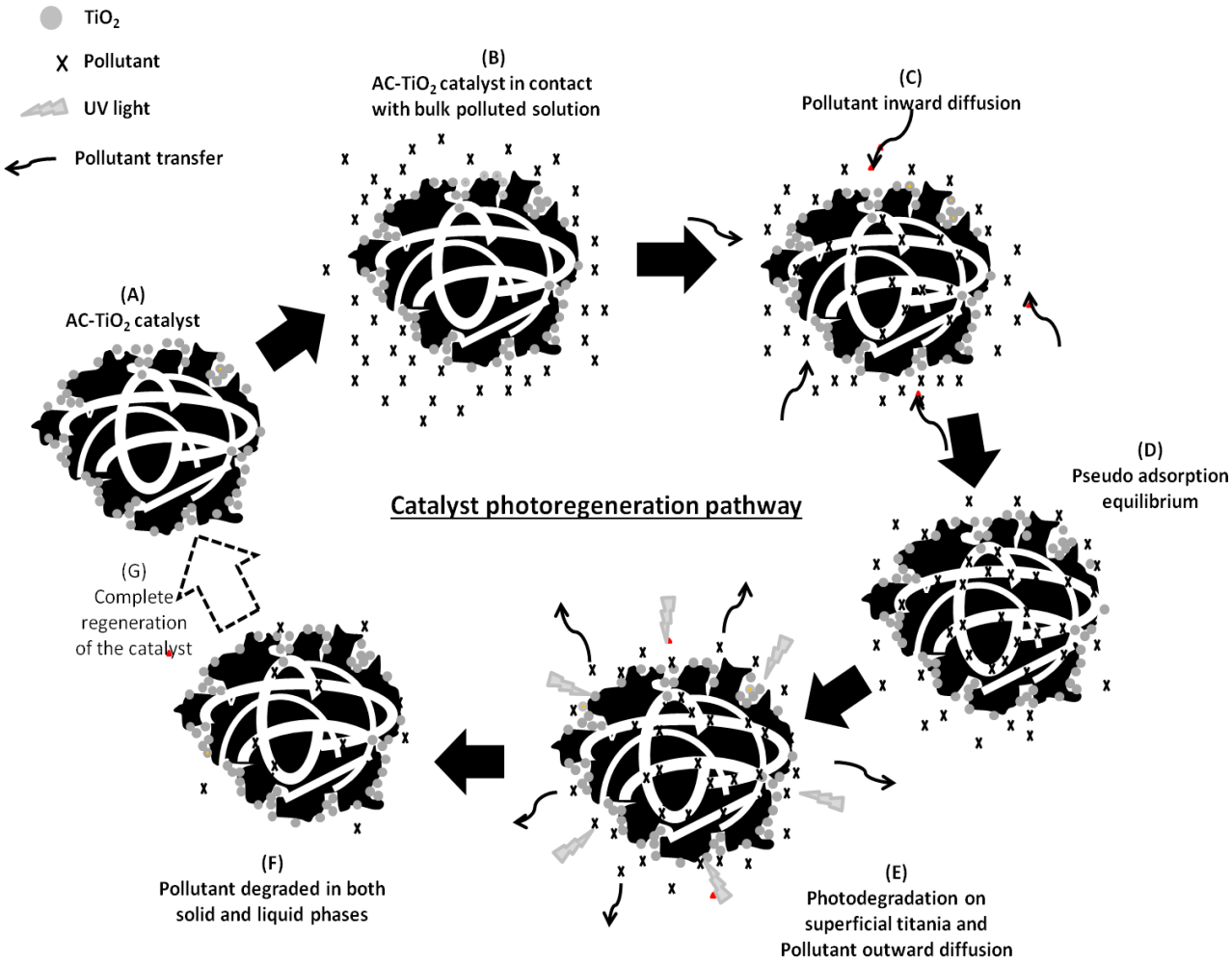

Fig. 7. Mechanism of phenol photoregeneration on TiO_2-AC catalyst with titania located on the surface macropores

Concluding remarks

Novel TiO_2 supported activated carbon catalysts were prepared by a straightforward titania coating route of activated carbon (AC) derived from tropical biomass. The proposed synthesis protocol enables a robust fixation of preformed titania anatase nanoparticles (TiO_2 NPs) in the external carbon porosity allowing their accessibility towards UV irradiation, without causing any reduction of the AC specific area. The porous texture of the as-prepared TiO_2-AC materials exhibits both a microporosity deriving from the AC support and an additional mesoporosity associated to the TiO_2 NPs anchorage. These structural and textural features of the TiO_2-AC catalysts were favorable to the reach of both higher adsorption capacity than the starting AC and interesting photo-degradation performances. During batch reactor photocatalysis experiments, 97% elimination rate of phenol in an aqueous solution was attained with catalysts of titania contents ranging from 11 to 34 wt%. The photodegradation performances of the TiO_2-AC catalysts were maintained after three successive utilizations, without regeneration treatment. Based on these results, a novel phenol photodegradation pathway including a photo-assisted regeneration mechanism of the catalyst is proposed. This study demonstrates the ability to develop in a simple way a TiO_2-AC catalyst with a specific nanocomposite microstrucure favourable to efficient adsorption and photodegradation functionalities, making possible the self-regeneration of the catalyst. Such kind of catalysts could significantly contribute to the development of simple, sustainable and low-cost solar photocatalytic processes for water treatment in developing countries where biomass and sunshine resources are widely available and underexploited. Further investigations on the influence of specific key parameters (pH of the sol, annealing treatment) are under consideration in order to strengthen the TiO_2-AC anchorage and improve the catalyst stability. Moreover, modeling mechanisms regarding the coupled phenomena are currently being studied in order to define the best way of implementing such materials for treating water in sunny areas of subsaharian Africa.

Acknowledgements

This work was financially supported by CIRAD and the SCAC program of the French embassy in Yaoundé-Cameroon. The authors are grateful to Odilon Changotade (2iE), Gilles Hernandez, Yonko Gorand, Eric Bèche, Danielle Perarnau (PROMES-CNRS), Cyril Vallicari (IEM), Ghislaine Volle and Jeremy Valette (CIRAD) for their great respective support on materials characterization. Special thanks are also extended to Anne Julbe and André Ayral for fruitful discussions and for providing the commercial titania sol.

References

1. Klavarioti M, Mantzavinos D, Kassinos D (2009) Removal of residual pharmaceuticals from aqueous systems by advanced oxidation processes. Environ Int 35:402–417. doi: 10.1016/j.envint.2008.07.009

2. Muthukumar M, Sargunamani D, Selvakumar N, Venkata Rao J (2004) Optimisation of ozone treatment for colour and COD removal of acid dye effluent using central composite design experiment. Dyes Pigments 63:127–134. doi: 10.1016/j.dyepig.2004.02.003

3. Hoffmann MR, Martin ST, Choi W, Bahnemann DW (1995) Environmental Applications of Semiconductor Photocatalysis. Chem Rev 95:69–96. doi: 10.1021/cr00033a004

4. Hisatomi T, Kubota J, Domen K (2014) Recent advances in semiconductors for photocatalytic and photoelectrochemical water splitting. Chem Soc Rev 43:7520–7535. doi: 10.1039/C3CS60378D

5. Plantard G, Janin T, Goetz V, Brosillon S (2012) Solar photocatalysis treatment of phytosanitary refuses: Efficiency of industrial photocatalysts. Appl Catal B Environ 115–116:38–44. doi: 10.1016/j.apcatb.2011.11.034

6. Daghrir R, Drogui P, Robert D (2013) Modified TiO2 For Environmental Photocatalytic Applications: A Review. Ind Eng Chem Res 52:3581–3599. doi: 10.1021/ie303468t

7. Fresno F, Portela R, Suárez S, Coronado JM (2014) Photocatalytic materials: recent achievements and near future trends. J Mater Chem A 2:2863–2884. doi: 10.1039/C3TA13793G

8. Fuentes KM, Betancourt P, Marrero S, García S (2017) Photocatalytic degradation of phenol using doped titania supported on photonic SiO2 spheres. React Kinet Mech Catal 120:403–415. doi: 10.1007/s11144-016-1097-3

9. Khan H (2017) Sol–gel synthesis of TiO2 from TiOSO4: characterization and UV photocatalytic activity for the degradation of 4-chlorophenol. React Kinet Mech Catal 121:811–832. doi: 10.1007/s11144-017-1195-x

10. Leary R, Westwood A (2011) Carbonaceous nanomaterials for the enhancement of TiO2 photocatalysis. Carbon 49:741–772. doi: 10.1016/j.carbon.2010.10.010

11. Matos J, Laine J, Herrmann J-M (1998) Synergy effect in the photocatalytic degradation of phenol on a suspended mixture of titania and activated carbon. Appl Catal B Environ 18:281–291. doi: 10.1016/S0926-3373(98)00051-4

12. Liu SX, Chen XY, Chen X (2007) A TiO2/AC composite photocatalyst with high activity and easy separation prepared by a hydrothermal method. J Hazard Mater 143:257–263. doi: 10.1016/j.jhazmat.2006.09.026

13. Wang X, Hu Z, Chen Y, et al (2009) A novel approach towards high-performance composite photocatalyst of TiO2 deposited on activated carbon. Appl Surf Sci 255:3953–3958. doi: 10.1016/j.apsusc.2008.10.083

14. Liu C, Li Y, Xu P, et al (2015) Controlled synthesis of ordered mesoporous TiO2-supported on activated carbon and pore-pore synergistic photocatalytic performance. Mater Chem Phys 149–150:69–76. doi: 10.1016/j.matchemphys.2014.09.034

15. Asenjo NG, Santamaría R, Blanco C, et al (2013) Correct use of the Langmuir–Hinshelwood equation for proving the absence of a synergy effect in the photocatalytic degradation of phenol on a suspended mixture of titania and activated carbon. Carbon 55:62–69. doi: 10.1016/j.carbon.2012.12.010

16. Cordero T, Duchamp C, Chovelon J-M, et al (2007) Influence of L-type activated carbons on photocatalytic activity of TiO2 in 4-chlorophenol photodegradation. J Photochem Photobiol Chem 191:122–131. doi: 10.1016/j.jphotochem.2007.04.012

17. Lim T-T, Yap P-S, Srinivasan M, Fane AG (2011) TiO2/AC Composites for Synergistic Adsorption-Photocatalysis Processes: Present Challenges and Further Developments for Water Treatment and Reclamation. Crit Rev Environ Sci Technol 41:1173–1230. doi: 10.1080/10643380903488664

18. Sengele A, Robert D, Keller N, et al (2016) Ta-doped TiO2 as photocatalyst for UV-A activated elimination of chemical warfare agent simulant. J Catal 334:129–141. doi: 10.1016/j.jcat.2015.11.004

19. Méndez-Medrano MG, Kowalska E, Lehoux A, et al (2016) Surface Modification of TiO2 with Ag Nanoparticles and CuO Nanoclusters for Application in Photocatalysis. J Phys Chem C 120:5143–5154. doi: 10.1021/acs.jpcc.5b10703

20. Baransi K, Dubowski Y, Sabbah I (2012) Synergetic effect between photocatalytic degradation and adsorption processes on the removal of phenolic compounds from olive mill wastewater. Water Res 46:789–798. doi: 10.1016/j.watres.2011.11.049

21. Liu W, Ni J, Yin X (2014) Synergy of photocatalysis and adsorption for simultaneous removal of Cr(VI) and Cr(III) with TiO2 and titanate nanotubes. Water Res 53:12–25. doi: 10.1016/j.watres.2013.12.043

22. Matos J, Montaña R, Rivero E (2014) Influence of activated carbon upon the photocatalytic degradation of methylene blue under UV–vis irradiation. Environ Sci Pollut Res 22:784–791. doi: 10.1007/s11356-014-2832-9

23. Velasco LF, Parra JB, Ania CO (2010) Role of activated carbon features on the photocatalytic degradation of phenol. Appl Surf Sci 256:5254–5258. doi: 10.1016/j.apsusc.2009.12.113

24. Chekem CT, Richardson Y, Plantard G, et al (2016) From Biomass Residues to Titania Coated Carbonaceous Photocatalysts: A Comparative Analysis of Different Preparation Routes for

Water Treatment Application. Waste Biomass Valorization 1–13. doi: 10.1007/s12649-016-9789-5

25. Ding Z, Hu X, Yue PL, et al (2001) Synthesis of anatase TiO2 supported on porous solids by chemical vapor deposition. Catal Today 68:173–182. doi: 10.1016/S0920-5861(01)00298-X

26. El-Sheikh AH, Newman AP, Al-Daffaee H, et al (2004) Deposition of anatase on the surface of activated carbon. Surf Coat Technol 187:284–292. doi: 10.1016/j.surfcoat.2004.03.012

27. Lettmann C, Hildenbrand K, Kisch H, et al (2001) Visible light photodegradation of 4-chlorophenol with a coke-containing titanium dioxide photocatalyst. Appl Catal B Environ 32:215–227. doi: 10.1016/S0926-3373(01)00141-2

28. Li Y, Zhang S, Yu Q, Yin W (2007) The effects of activated carbon supports on the structure and properties of TiO2 nanoparticles prepared by a sol–gel method. Appl Surf Sci 253:9254–9258. doi: 10.1016/j.apsusc.2007.05.057

29. Yuan R, Guan R, Zheng J (2005) Effect of the pore size of TiO2-loaded activated carbon fiber on its photocatalytic activity. Scr Mater 52:1329–1334. doi: 10.1016/j.scriptamat.2005.02.028

30. Liang Y, Wang H, Casalongue HS, et al (2010) TiO2 nanocrystals grown on graphene as advanced photocatalytic hybrid materials. Nano Res 3:701–705. doi: 10.1007/s12274-010-0033-5

31. Subramani AK, Byrappa K, Ananda S, et al (2007) Photocatalytic degradation of indigo carmine dye using TiO2 impregnated activated carbon. Bull Mater Sci 30:37–41. doi: 10.1007/s12034-007-0007-8

32. Velasco LF, Tsyntsarski B, Petrova B, et al (2010) Carbon foams as catalyst supports for phenol photodegradation. J Hazard Mater 184:843–848. doi: 10.1016/j.jhazmat.2010.08.118

33. Kadirova ZC, Hojamberdiev M, Katsumata K, et al (2013) Photodegradation of gaseous acetaldehyde and methylene blue in aqueous solution with titanium dioxide-loaded activated carbon fiber polymer materials and aquatic plant ecotoxicity tests. Environ Sci Pollut Res 1–11. doi: 10.1007/s11356-013-2405-3

34. Gar Alalm M, Tawfik A, Ookawara S (2016) Enhancement of photocatalytic activity of TiO2 by immobilization on activated carbon for degradation of pharmaceuticals. J Environ Chem Eng 4:1929–1937. doi: 10.1016/j.jece.2016.03.023

35. Mohd Din AT, Hameed BH, Ahmad AL (2009) Batch adsorption of phenol onto physiochemical-activated coconut shell. J Hazard Mater 161:1522–1529. doi: 10.1016/j.jhazmat.2008.05.009

36. Kahru A, Pollumaa L, Reiman R, et al (2000) The toxicity and biodegradability of eight main phenolic compounds characteristic to the oil-shale industry wastewaters: A test battery approach - Kahru - 2000 - Environmental Toxicology - Wiley Online Library. Environ Toxicol 15:431–442.

37. Salame II, Bandosz TJ (2003) Role of surface chemistry in adsorption of phenol on activated carbons. J Colloid Interface Sci 264:307–312. doi: 10.1016/S0021-9797(03)00420-X

38. Noumi ES, Dabat M-H, Blin J (2013) Energy efficiency and waste reuse: A solution for sustainability in poor West African countries? Case study of the shea butter supply chain in Burkina Faso. J Renew Sustain Energy 5:53134. doi: 10.1063/1.4824432

39. Itodo AU, Itodo HU, Gafar MK (2010) Evaluation of Dyestuff Removal by Shea Nut (Vitellaria paradoxa) shells. J Appl Sci Environ Manag. doi: 10.4314/jasem.v14i4.63309

40. Réti B, Mogyorósi K, Dombi A, Hernádi K (2014) Substrate dependent photocatalytic performance of TiO2/MWCNT photocatalysts. Appl Catal Gen 469:153–158. doi: 10.1016/j.apcata.2013.10.001

41. Tryba B, Morawski AW, Inagaki M, Toyoda M (2006) Effect of the carbon coating in Fe-C-TiO(2) photocatalyst on phenol decomposition under UV irradiation via photo-Fenton process. Chemosphere 64:1225–1232. doi: 10.1016/j.chemosphere.2005.11.035

42. Cheng G, Stadler FJ (2015) Achieving phase transformation and structure control of crystalline anatase TiO2@C hybrids from titanium glycolate precursor and glucose molecules. J Colloid Interface Sci 438:169–178. doi: 10.1016/j.jcis.2014.09.084

43. ZENG M, LI Y, MA M, et al (2013) Photocatalytic activity and kinetics for acid yellow degradation over surface composites of TiO2-coated activated carbon under different photocatalytic conditions. Trans Nonferrous Met Soc China 23:1019–1027. doi: 10.1016/S1003-6326(13)62561-3

44. Noh JS, Schwarz JA (1989) Estimation of the point of zero charge of simple oxides by mass titration. J Colloid Interface Sci 130:157–164. doi: 10.1016/0021-9797(89)90086-6

45. Liu Y, Yang S, Hong J, Sun C (2007) Low-temperature preparation and microwave photocatalytic activity study of TiO2-mounted activated carbon. J Hazard Mater 142:208–215. doi: 10.1016/j.jhazmat.2006.08.020

46. El-Sheikh AH, Al-Degs YS, Newman AP, Lynch DE (2007) Oxidized activated carbon as support for titanium dioxide in UV-assisted degradation of 3-chlorophenol. Sep Purif Technol 54:117–123. doi: 10.1016/j.seppur.2006.08.020

47. Carpio E, Zúñiga P, Ponce S, et al (2005) Photocatalytic degradation of phenol using TiO2 nanocrystals supported on activated carbon. J Mol Catal Chem 228:293–298. doi: 10.1016/j.molcata.2004.09.066

48. Lente G (2015) Deterministic Kinetics in Chemistry and Systems Biology The Dynamics of Complex Reaction Networks. Springer

49. Ahmaruzzaman M, Sharma DK (2005) Adsorption of phenols from wastewater. J Colloid Interface Sci 287:14–24. doi: 10.1016/j.jcis.2005.01.075

50. Gueye M, Richardson Y, Kafack FT, Blin J (2014) High efficiency activated carbons from African biomass residues for the removal of chromium(VI) from wastewater. J Environ Chem Eng 2:273–281. doi: 10.1016/j.jece.2013.12.014

51. Molina-Sabio M, Rodríguez-Reinoso F (2004) Role of chemical activation in the development of carbon porosity. Colloids Surf Physicochem Eng Asp 241:15–25. doi: 10.1016/j.colsurfa.2004.04.007

52. Zhang X, Zhou M, Lei L (2005) Preparation of photocatalytic TiO2 coatings of nanosized particles on activated carbon by AP-MOCVD. Carbon 43:1700–1708. doi: 10.1016/j.carbon.2005.02.013

53. Hanaor DAH, Sorrell CC (2011) Review of the anatase to rutile phase transformation. J Mater Sci 46:855–874. doi: 10.1007/s10853-010-5113-0

54. Wetchakun N, Incessungvorn B, Wetchakun K, Phanichphant S (2012) Influence of calcination temperature on anatase to rutile phase transformation in TiO2 nanoparticles synthesized by the modified sol–gel method. Mater Lett 82:195–198. doi: http://dx.doi.org/10.1016/j.matlet.2012.05.092

55. Favaro M, Agnoli S, Di Valentin C, et al (2014) TiO2/graphene nanocomposites from the direct reduction of graphene oxide by metal evaporation. Carbon 68:319–329. doi: 10.1016/j.carbon.2013.11.008

56. Carp O, Huisman CL, Reller A (2004) Photoinduced reactivity of titanium dioxide. Prog Solid State Chem 32:33–177. doi: 10.1016/j.progsolidstchem.2004.08.001

57. Zhang Z, Wang C-C, Zakaria R, Ying JY (1998) Role of Particle Size in Nanocrystalline TiO2-Based Photocatalysts. J Phys Chem B 102:10871–10878. doi: 10.1021/jp982948+

58. Py X, Guillot A, Cagnon B (2003) Activated carbon porosity tailoring by cyclic sorption/decomposition of molecular oxygen. Carbon 41:1533–1543. doi: 10.1016/S0008-6223(03)00092-7

59. Araña J, Doña-Rodríguez JM, Tello Rendón E, et al (2003) TiO2 activation by using activated carbon as a support: Part II. Photoreactivity and FTIR study. Appl Catal B Environ 44:153–160. doi: 10.1016/S0926-3373(03)00075-4

60. Roostaei N, Tezel FH (2004) Removal of phenol from aqueous solutions by adsorption. J Environ Manage 70:157–164. doi: 10.1016/j.jenvman.2003.11.004

61. Tancredi N, Medero N, Möller F, et al (2004) Phenol adsorption onto powdered and granular activated carbon, prepared from Eucalyptus wood. J Colloid Interface Sci 279:357–363. doi: 10.1016/j.jcis.2004.06.067

62. Gianluca Li Puma AB (2008) Preparation of titanium dioxide photocatalyst loaded onto activated carbon support using chemical vapor deposition: a review paper. J Hazard Mater 157:209–19. doi: 10.1016/j.jhazmat.2008.01.040

63. Yuan R, Guan R, Liu P, Zheng J (2007) Photocatalytic treatment of wastewater from paper mill by TiO2 loaded on activated carbon fibers. Colloids Surf Physicochem Eng Asp 293:80–86. doi: 10.1016/j.colsurfa.2006.07.010

64. Li Y, Li X, Li J, Yin J (2006) Photocatalytic degradation of methyl orange by TiO2-coated activated carbon and kinetic study. Water Res 40:1119–1126. doi: 10.1016/j.watres.2005.12.042

65. Sobczyński A, Duczmal Ł, Zmudziński W (2004) Phenol destruction by photocatalysis on TiO2: an attempt to solve the reaction mechanism. J Mol Catal Chem 213:225–230. doi: 10.1016/j.molcata.2003.12.006

66. Quintanilla A, Casas JA, Mohedano AF, Rodríguez JJ (2006) Reaction pathway of the catalytic wet air oxidation of phenol with a Fe/activated carbon catalyst. Appl Catal B Environ 67:206–216. doi: 10.1016/j.apcatb.2006.05.003

67. Gamage McEvoy J, Cui W, Zhang Z (2014) Synthesis and characterization of Ag/AgCl–activated carbon composites for enhanced visible light photocatalysis. Appl Catal B Environ 144:702–712. doi: 10.1016/j.apcatb.2013.07.062

68. Matos J, Laine J, Herrmann J-M (2001) Effect of the Type of Activated Carbons on the Photocatalytic Degradation of Aqueous Organic Pollutants by UV-Irradiated Titania. J Catal 200:10–20. doi: 10.1006/jcat.2001.3191

69. Goetz V, Cambon JP, Sacco D, Plantard G (2009) Modeling aqueous heterogeneous photocatalytic degradation of organic pollutants with immobilized TiO2. Chem Eng Process Process Intensif 48:532–537. doi: 10.1016/j.cep.2008.06.013

70. Zekri M el M, Colbeau-Justin C (2013) A mathematical model to describe the photocatalytic reality: What is the probability that a photon does its job? Chem Eng J 225:547–557. doi: 10.1016/j.cej.2013.03.129

71. Terzyk AP (2003) Further insights into the role of carbon surface functionalities in the mechanism of phenol adsorption. J Colloid Interface Sci 268:301–329. doi: 10.1016/S0021-9797(03)00690-8

Effective coupling of phenol adsorption and photodegradation at the surface of micro-and mesoporous TiO_2-activated carbon materials

C. Telegang Chekem[(1)(2)],Y. Richardson[(1)], M. Drobek[(3)],G. Plantard[(2)], J. Blin[(1)(4)], V. Goetz[(2)]

[(1)]Institut International d'Ingénierie de l'Eau et de l'Environnement (2iE), Laboratoire Biomasse Energie et Biocarburants (LBEB), Rue de la Science, 01 BP 594, Ouagadougou 01, Burkina Faso

[(2)]PROMES-CNRS UPR 8521, PROcess Material and Solar Energy, Rambla de la Thermodynamique 66100 Perpignan, France

[(3)]Institut Européen des Membranes, UMR 5635, Université de Montpellier, ENSCM, CNRS, Place Eugène Bataillon, F-34095 Montpellier cedex 5, France

[(4)] CIRAD, UPR BioWooEB, F-34398 Montpellier, France

Supplementary Information

Table S1 Ultimate and proximate analysis of shea nut shell (SNS) and derived AC

Properties	Content (wt %)	
	SNS	**AC**
Ash	3.82	6.52
Volatiles	74.11	13.87
Fixed carbon	22.07	79.61
C	49.21	75.38
H	6.09	1.79
O[a]	44.52	22.42
N	0.18	0.41

[a]Calculated by difference

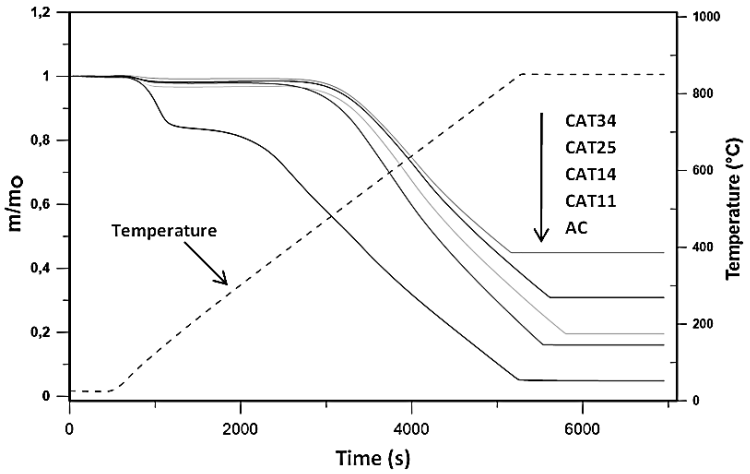

Fig. S1 TGA mass variation of uncoated AC and CATx catalysts

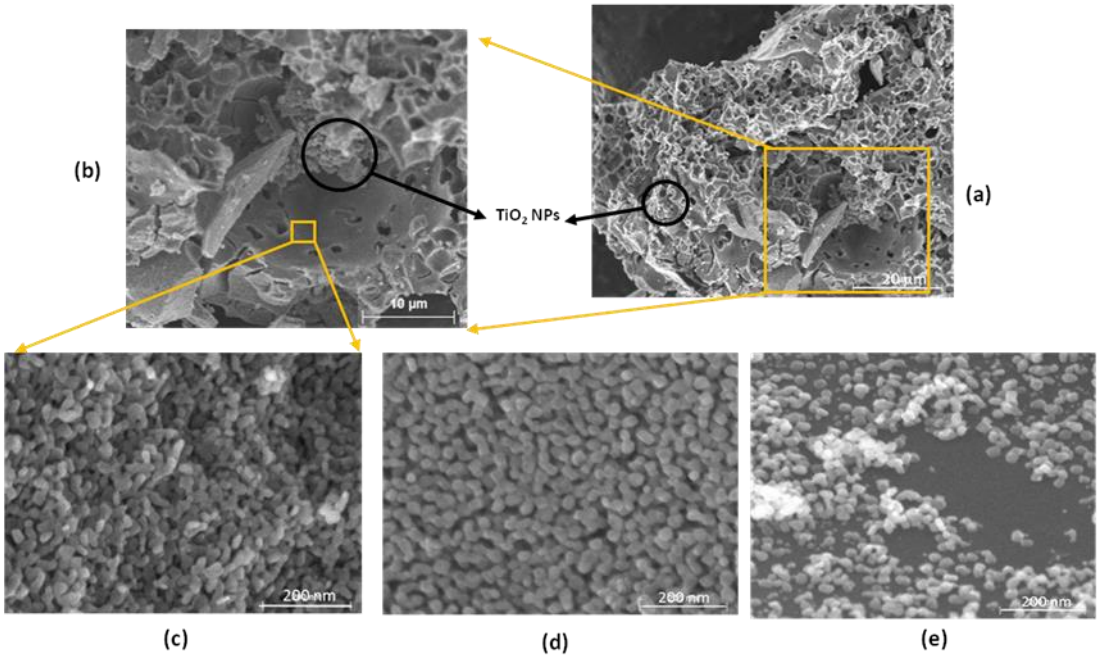

Fig. S2 FESEM images of AC-TiO_2 catalysts. a, b and c : *CAT34*; d : *CAT25* ; e : *CAT11*. *CATX* is a catalyst obtained with *X* % wt/wt titania

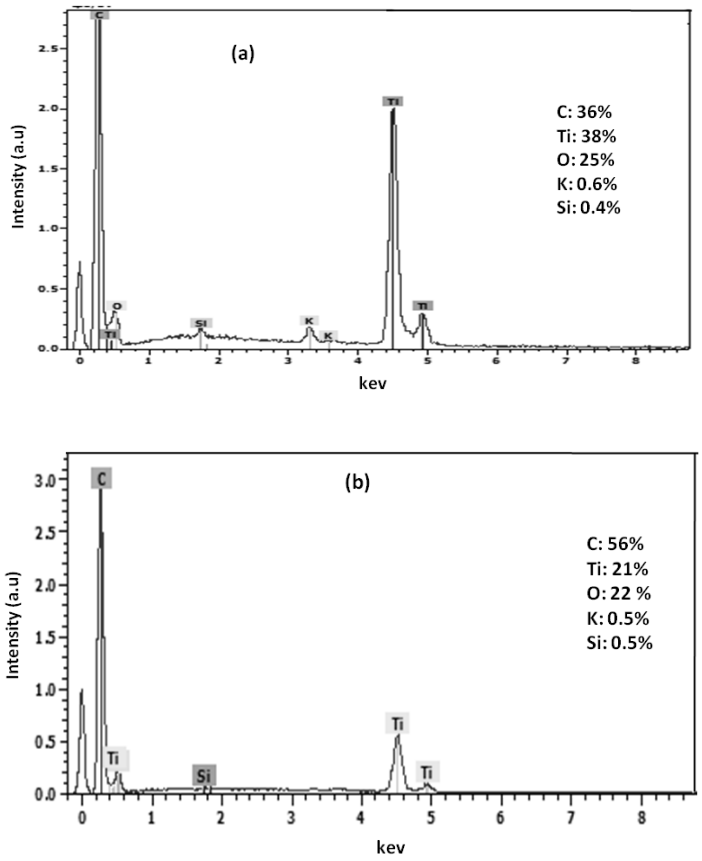

Fig. S3 EDX spectra on (a) CAT34 and (b) CAT25

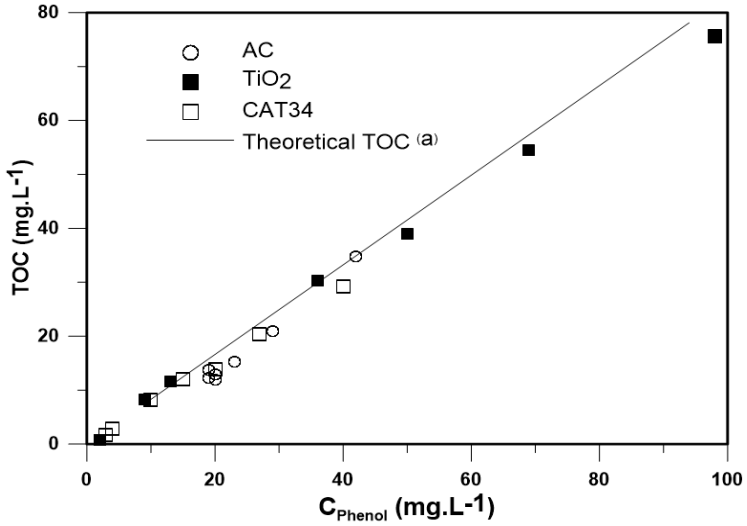

Fig. S4 Variation of COT against phenol concentration with different materials. [(a)]Calculated based on the carbon content of phenol molecule